



# Damage and polymerization of C<sub>60</sub> films irradiated by fast light and heavy ions

A. Yogo, T. Majima, A. Itoh \*

*Quantum Science and Engineering Center, Kyoto University, Kyoto 606-8501, Japan*

## Abstract

C<sub>60</sub> films have been irradiated with various fast ions (H, Li, C, O and Si) in the energy range from 0.75 to 6.0 MeV. Structural changes of C<sub>60</sub> molecules were studied by a time-of-flight (TOF) mass spectrometry and Raman spectroscopy. The TOF yields of secondary fullerene ions can be described fairly well by  $S_{\text{mod}}^3$  with a modified energy deposition  $S_{\text{mod}}$  developed in this work. In the Raman study for 1 MeV H<sup>+</sup> irradiation, it is found that about 40% polymerization is attained at  $6 \times 10^{15} \text{ cm}^{-2}$  doses and a damage cross-section of  $2.5 \times 10^{-17} \text{ cm}^2$  is obtained. © 2002 Elsevier Science B.V. All rights reserved.

PACS: 79.20.Ne

Keywords: Fullerene polymer; C<sub>60</sub> films; Secondary ion emission; Ion irradiation

## 1. Introduction

The macroscopic availability of fullerene, the third allotropic form of carbon, has opened broad application fields of carbonaceous frontier materials ranging from surface lubricator to non-linear optical devices [1]. Since the first discovery of polymerized C<sub>60</sub> films [2], there has been a surge of interest in fullerene polymers, including several techniques of polymerization such as photo-irradiation [3], high-pressure high-temperature (HPHT) processing [4], alkali-metal doping [1] and so on. It has been established both experimentally and theoretically that C<sub>60</sub> molecules are

bound to each other via one kind of covalent bond called [2 + 2] cycloadditional four-membered rings [2].

However, there are few investigations focusing on the polymerization of C<sub>60</sub> films induced by ion irradiation. This is because bombardment of fullerene by energetic particles is accompanied by the destruction of fullerene-cage structure, which makes the phenomenon more complicated. For instance, a Raman study of C<sub>60</sub> films irradiated by a few hundreds keV ions [5] shows that the increase of irradiation doses promotes polymerization of C<sub>60</sub> molecules and at higher doses, on the contrary, the polymerization intensity starts to decrease. Similar results are obtained for swift heavy ion irradiations at energies above 1.7 MeV/amu, where the processes are mainly governed by electronic mechanisms [6]. On the other hand, little information is available about electronic

\* Corresponding author. Tel.: +81-75-753-5828; fax: +81-75-753-3751.

E-mail address: [itoh@nucleng.kyoto-u.ac.jp](mailto:itoh@nucleng.kyoto-u.ac.jp) (A. Itoh).

interactions between a solid-state  $C_{60}$  and swift ions due to the lack of understanding of the energy transport process inside a solid.

In this paper a comprehensive investigation is performed of the swift ion irradiation effect on fullerene  $C_{60}$  films by using a time-of-flight (TOF) mass spectrometry to investigate secondary cluster ions sputtered electronically from a pristine  $C_{60}$  surface, and Raman spectroscopy to evaluate damage and polymerization of bulked  $C_{60}$  molecules.

## 2. Experimental

The experiment was performed at the 1.7 MeV tandem Cockcroft–Walton accelerator facility of Kyoto University. Beams of  $^1H^+$ ,  $^7Li^{q+}$ ,  $^{12}C^{q+}$ ,  $^{16}O^{q+}$  and  $^{28}Si^{q+}$  ( $q = 1-4$ ) are used.  $C_{60}$  thin films were prepared on a Si(111) substrate by sublimation of 99.98% pure powder at 450 °C in a vacuum chamber below  $8 \times 10^{-7}$  Torr. The powder was well degassed in vacuum at 300 °C for more than 10 h in order to remove residual organic solvents from the powder. Thickness of the  $C_{60}$  films is about 1  $\mu m$ , which is shorter than the range of the projectile ions. It is worth noting that the  $C_{60}$  films prepared in this way have a nanocrystalline-fcc structure with a typical grain size of 10–20 nm [1].

The TOF measurement was performed by a beam-chopping method described in [7] with a frequency of 10 kHz and a 50 ns width. Secondary ions emitted from a  $C_{60}$  film surface were extracted by an electrostatic field of 16.7 V/mm toward a channel electron multiplier. A flight time of  $C_{60}$  ions was about 12  $\mu s$ .

$C_{60}$  films used for Raman study were irradiated by 1 MeV  $H^+$  with doses between  $6 \times 10^{12}$  and  $6 \times 10^{16}$   $cm^{-2}$ . The beam current was kept below 200 nA to avoid heating of the samples [8]. The beam direction was normal to the target surface. The Raman measurement was carried out with a microscope-laser-Raman assembly, using an Ar ion laser (514.5 nm) with a minimum laser power of 5  $mW/mm^2$  to avoid excitation effects of light [8].

## 3. Results and discussion

Fig. 1 shows a typical TOF spectrum obtained for 2.3 MeV  $O^{2+}$  impacts. It is easily identified that the peaks corresponds to  $C_{60N}$  ( $N = 1-3$ ). Similar results were reported in [9]. It was found that the relative yields of the fullerene ions have changed significantly for different incident ions of Li, C, O and Si.

Yields of the secondary fullerene ions were analyzed by using the ‘effective energy deposition model’ developed by Pereira et al. [10,12]. According to this model, the energy density  $e(r)$  (eV/ $\text{\AA}^3$ ) deposited by the projectile is expressed by the following Lorentzian function,

$$e(r) = \begin{cases} \frac{\epsilon_0}{1+(r/r_i)^2} & \text{for } r \leq r_u, \\ 0 & \text{for } r > r_u, \end{cases} \quad (1)$$

where  $r$  is the distance from the ion trajectory,  $r_u$  and  $r_i$  are radii of ultratrack and infratrack [11], respectively, given by

$$r_i \approx 6.7(E/M)^{1/2} \quad \text{and} \quad r_u \approx 830(E/M)/\rho \quad (\text{\AA}), \quad (2)$$

where  $E$  the projectile energy (MeV),  $M$  the mass (amu) and  $\rho$  the target density ( $g/cm^3$ ). The electronic stopping power  $S_e$  is obtained by integrating  $e(r)$  over  $0 \leq r \leq r_u$ , giving rise to

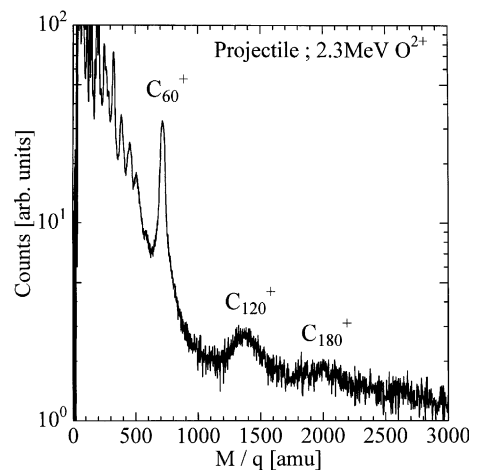


Fig. 1. A TOF spectrum obtained for 2.3 MeV  $O^{2+}$  impact on  $C_{60}$  films. It is easily identified that the peaks corresponds to  $C_{60N}$  ( $N = 1-3$ ).

$$\epsilon_0 = \frac{S_c}{\pi r_i^2 \ln[1 + (r_u/r_i)^2]} \quad (3)$$

Assuming that the emission of a secondary ion requires a certain energy density,  $\epsilon_c = e(r_c)$ , an effective energy deposition  $S_{\text{eff}}$  is described as

$$S_{\text{eff}} = \int_0^{r_c} 2\pi r e(r) dr = S_c \frac{\ln(\epsilon_0/\epsilon_c)}{\ln[1 + (r_u/r_i)^2]} \quad (4)$$

The value of  $\epsilon_c$  is used as a fitting parameter. Energy density distributions  $e(r)$  are shown in Fig. 2 for  $\text{O}^{q+}$  impacts. The ultratrack radii  $r_u$  are calculated to be 24 and 122 Å for 0.80 and 4.0 MeV  $\text{O}^{q+}$  impacts, respectively. One can see a surprising result that 0.80 MeV impacts deposits higher energy density near the ion trajectory than that of 4.0 MeV impacts.

In this model, it is assumed that the low energy density region does not contribute to the secondary ion emission, and  $S_{\text{eff}}$  is to be calculated within the critical regions. We improved this model in the following.

Zawislak et al. [8] reported that the destruction of  $\text{C}_{60}$  molecules by ion irradiation is completed at a deposited energy density larger than  $0.5 \text{ eV}/\text{Å}^3$ . Therefore, the inner region of the track with  $e(r) \geq 0.5 \text{ eV}/\text{Å}^3$  has no contribution to the

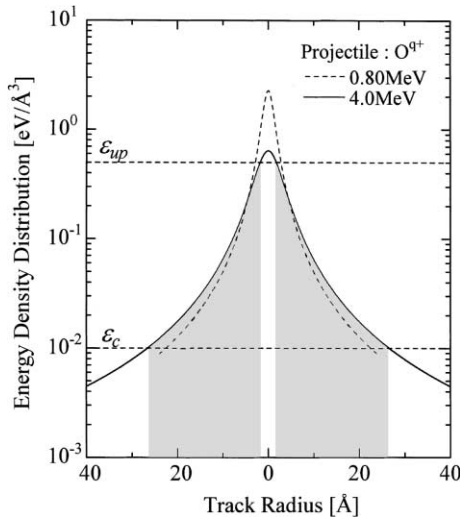


Fig. 2. Energy density distributions  $e(r)$  obtained for 0.8 and 4.0 MeV  $\text{O}^{q+}$  impact.  $S_{\text{mod}}$  is calculated by integrating the region between  $\epsilon_c$  and  $\epsilon_{\text{up}}$ .

emission of the fullerene ions such as  $\text{C}_{60}$  or  $\text{C}_{120}$ . Hence, the effective energy deposition  $S_{\text{eff}}$  for  $\text{C}_{60}$  films should be obtained by excluding the inner region. This new quantity is defined as ‘modified energy deposition’  $S_{\text{mod}}$  by

$$S_{\text{mod}} = \int_{r_{\text{up}}}^{r_c} 2\pi r e(r) dr = S_c \frac{\ln(\epsilon_{\text{up}}/\epsilon_c)}{\ln[1 + (r_u/r_i)^2]} \quad (5)$$

where  $\epsilon_{\text{up}} = e(r_{\text{up}}) = 0.5 \text{ eV}/\text{Å}^3$  represents an upper limit of the energy density contributing to the emission of fullerene ions. Using this  $S_{\text{mod}}$ , the yields of  $\text{C}_{60}$  and  $\text{C}_{120}$  ions are successfully expressed in a form of  $S_{\text{mod}}^3$  as demonstrated in Fig. 3. It is worth noting that this expression holds independently of the projectile velocity.

The critical energy density  $\epsilon_c$  was estimated to be  $0.01 \text{ eV}/\text{Å}^3$  for the emission of  $\text{C}_{60}$  and  $\text{C}_{120}$  ions. Assuming  $700 \text{ Å}^3$  as the volume per  $\text{C}_{60}$  molecule [8], the energy densities per  $\text{C}_{60}$  and  $\text{C}_{120}$  are estimated to be about 7 and 14 eV,

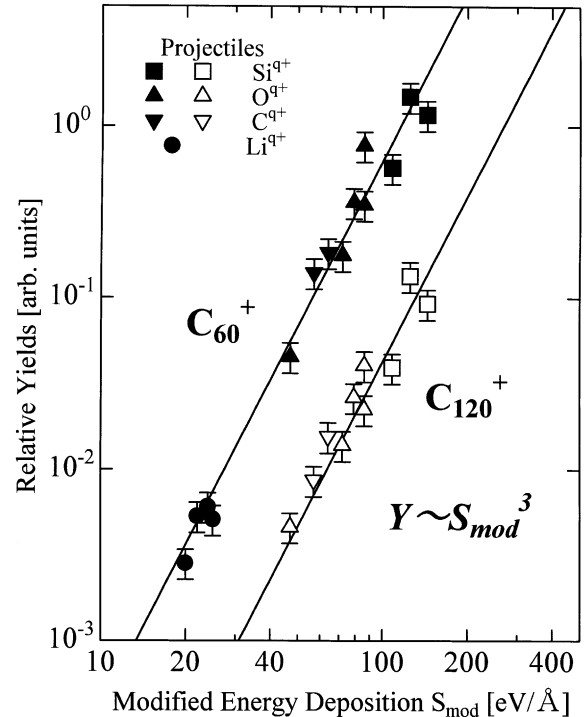


Fig. 3. Relative yields of fullerene ions versus modified stopping power  $S_{\text{mod}}$  ( $\text{eV}/\text{Å}$ ) calculated from Eq. (5). The yields are well described as  $Y \sim S_{\text{mod}}^3$ .

respectively. These values are fairly close to the following estimation: using the first ionization potential of  $C_{60}$  ( $I = 7.58$  eV) and the cohesive energy of  $C_{60}$  films ( $E_c = 1.6$  eV/ $C_{60}$ ), the energy necessary for the emission of  $C_{60}$  and  $C_{120}$  ions can be estimated to be  $I + E_c = 9$  eV and  $I + 2E_c = 11$  eV, respectively. The polymerization will need another few eV of energy per  $C_{60}$ . Therefore, it is concluded that the critical energy density  $\epsilon_c$  is determined appropriately for the emission of the fullerene ions.

The values of  $\epsilon_c$  and  $\epsilon_{up}$  provide another important information about the ion-track structure. It is possible to estimate the critical radius within which the emission of fullerene ions, like  $C_{60}$  and  $C_{120}$ , occurs. The emission region of the fullerene ions estimated in this way is a ‘donuts-shaped’ area around the projectile trajectory with inner radius of 1–5.5 Å and outer radius of 15–35 Å for Li, C, O and Si impacts.

The Raman spectra were obtained for non-irradiated and ion-irradiated films. It was observed that the intensity of Raman peaks becomes weaker as the dose increases. Especially, the tangential ‘‘pentagonal pinch’’ mode  $A_g(2)$  is significantly weakened and broadened after the irradiation. The  $A_g(2)$  mode has proven to be a particularly reliable probe of the polymerization state, because the shift of this mode is very sensitive to the number of covalent bonds of  $C_{60}$  [13]. Thus, the  $A_g(2)$  mode was carefully analyzed as described in the following.

Fig. 4 shows Raman spectra around the  $A_g(2)$  mode for irradiation doses of  $6 \times 10^{15}$  and  $6 \times 10^{16}$   $\text{cm}^2$ .  $H_g(7)$  in the figure corresponds to another vibration mode of  $C_{60}$  molecules. The experimental data were successfully fitted by Voigt functions, resulting in the resolution of the  $A_g(2)$  mode into six individual components positioned at 1470, 1466, 1460, 1453, 1444 and 1433  $\text{cm}^{-1}$ . It is known that the  $A_g(2)$  mode shifts in proportion to the number of intermolecular covalent bonds [14], and the formation of dimers results in a shift of about 5  $\text{cm}^{-1}$  [13]. Hence, it is concluded that the fitted components at 1466, 1460, 1444 and 1433  $\text{cm}^{-1}$  obtained in our experiments may certainly correspond to dimers, linear chains, tetragonal plains and rhombohedral plains [4], respectively. In ad-

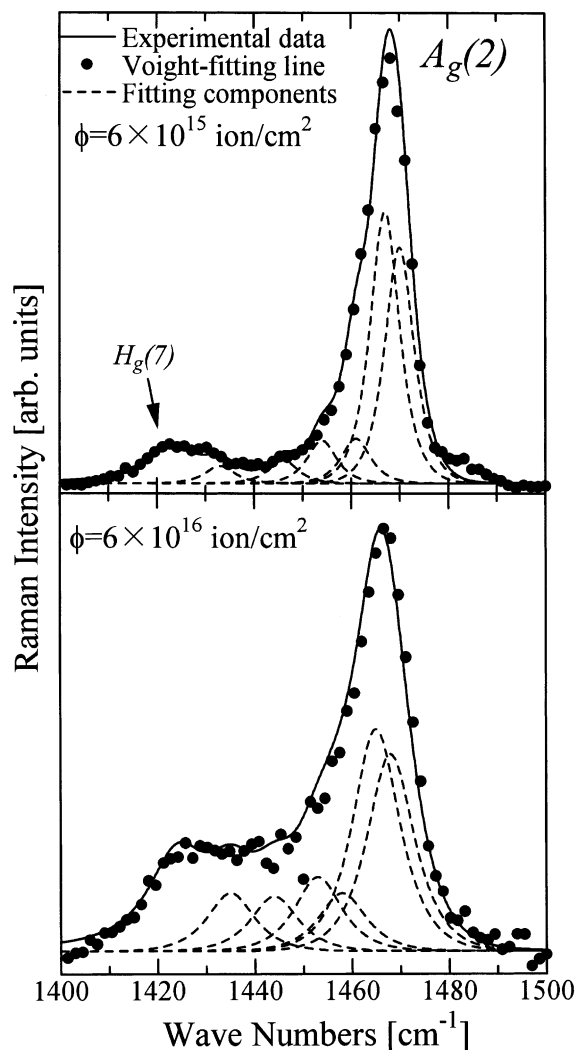


Fig. 4. The Raman spectra between 1400 and 1500  $\text{cm}^{-1}$  taken at doses of  $6 \times 10^{15}$  and  $6 \times 10^{16}$   $\text{cm}^{-2}$ , showing  $A_g(2)$  vibration mode. The dotted curves represent individual fitted components by Voigt functions.

dition, we found that the polymer components occupies about 70% area of the broadened  $A_g(2)$  peak for the films of  $6 \times 10^{16}$   $\text{cm}^{-2}$  doses.

The damage process of  $C_{60}$  films was investigated by measuring the peak intensities of  $A_g(2)$ . Fig. 5 shows survival ratios and polymerized ratios of the  $C_{60}$  films as a function of the irradiation dose  $\phi$ . The survival ratio is obtained from the relative intensity of  $A_g(2)$  mode, including the polymer components mentioned above. Hence, the survival

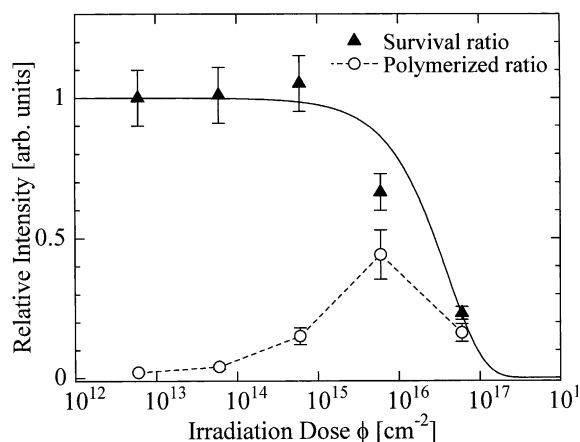


Fig. 5. Survival and polymerized ratio of  $\text{C}_{60}$  molecules in the films as a function of the irradiation dose,  $\phi$  ( $\text{cm}^{-2}$ ).

ratio represents the fraction of intact  $\text{C}_{60}$  molecules in the films, of either isolated or polymerized. By fitting the survival ratio to an exponential curve,  $I/I_0 = \exp(-\sigma\phi)$ , the damage cross-section of  $\sigma = 2.5 \times 10^{-17} \text{cm}^2$  is obtained for the 1 MeV  $\text{H}^+$  irradiation. This value coincides reasonably with the FT-IR results obtained using MeV energy heavy ion irradiation [15], where a damage cross-section is estimated to be about  $1 \times 10^{-16} \text{cm}^2$  for 2.5 MeV  $\text{He}^+$  impacts.

The polymerization ratio shown in Fig. 5 is obtained from a summation over the polymer components. The fraction reaches a maximum at about  $6 \times 10^{15} \text{cm}^{-2}$  doses. This result means that the polymerization process is dominant at lower doses and the damaging effect becomes significant at higher doses. Hence, the damage cross-section may be smaller than that of the polymerization. In other words, the polymerization occurs in relatively broader region around the projectile. This assumption coincides with previous discussions about  $S_{\text{mod}}$ , where ions are expected to be emitted from donuts-shaped regions around the projectile.

#### 4. Summary

The swift ion irradiation effects on fullerene  $\text{C}_{60}$  films are studied by using TOF mass spectrometry and Raman spectroscopy.

In the TOF study the yields of secondary fullerene ions, such as  $\text{C}_{60}$  and were analyzed by the modified energy deposition  $S_{\text{mod}}$ , developed newly in this work. Yields of the fullerene ions are expressed fairly well in the form of  $S_{\text{mod}}^3$ . The effective region contributing to the emission of fullerene ions is also estimated to be a donuts-shaped area around the projectile trajectory with inner radius of the order of  $\text{\AA}$  and outer radius of a few nm for Li, C, O and Si impacts.

In the Raman study the  $A_g(2)$  vibration mode was analyzed extensively, leading to a finding of fullerene polymers induced by the 1 MeV  $\text{H}^+$  irradiation. It is also found that the intensity of polymerization reaches a maximum at about  $6 \times 10^{15} \text{cm}^{-2}$ , at which about 40% of the film is polymerized. The damage cross-section is estimated to be  $\sigma = 2.5 \times 10^{-17} \text{cm}^2$ , which is quite smaller than the geometrical cross-section of  $\text{C}_{60}$  molecules.

#### Acknowledgements

We gratefully acknowledge Dr. K. Takahiro and Dr. K. Kawatsura at Kyoto Institute of Technology for the cooperation in the Raman experiment. We also thank K. Yoshida, Y. Hamamoto and F. Obata for their help during the TOF experiment.

#### References

- [1] M.S. Dresselhaus, G. Dresselhaus, P.C. Eklund, Science of Fullerenes and Carbon Nanochubes, Academic Press, New York, 1996.
- [2] A.M. Rao, P. Zhou, K. Wang, G. Hager, J.M. Holden, Y. Wang, W.T. Lee, X. Bi, P.C. Eklund, D.S. Cornett, M.A. Duncan, I.J. Amster, Science 259 (1993) 955.
- [3] J. Onoe, A. Nakao, K. Takeuchi, Phys. Rev. B 55 (1997) 10051.
- [4] A.M. Rao, P.C. Eklund, J-L. Hodeau, L. Marques, M. Nunez-Regueiro, Phys. Rev. B 55 (1997) 4766.
- [5] L. Palmethofer, J. Kastner, Nucl. Instr. and Meth. B 96 (1995) 343.
- [6] S. Lotha, A. Ingale, D.K. Avasthi, V.K. Mittal, S. Mishra, K.C. Rustagi, A. Gupta, V.N. Kulkarni, D.T. Khathing, Solid State Commun. 111 (1999) 55.

- [7] A. Itoh, H. Tsuchida, T. Majima, S. Anada, A. Yogo, N. Imanishi, *Phys. Rev. B* 61 (1999) 012702.
- [8] F.C. Zawislak, D.L. Baptista, M. Behar, D. Fink, P.L. Grande, J.A.H. da Jornada, *Nucl. Instr. and Meth. B* 149 (1999) 336.
- [9] R.M. Papaléo, P.A. Demirev, J. Eriksson, P. Håkansson, B.U.R. Sundqvist, *Int. J. Mass Spectrosc. Ion Proc.* 152 (1996) 193.
- [10] J.A.M. Pereira, I.S. Bitensky, E.F. da Silveira, *Int. J. Mass Spectrosc. Ion Proc.* 174 (1998) 179.
- [11] P. Håkansson, *K. Dan. Vidensk. Selsk. Mat. Fys. Medd.* 43 (1993) 93.
- [12] R. Neugebauer, J.A.M. Pereira, R. Wunsch, T. Jalowy, K.O. Groeneveld, *Nucl. Instr. and Meth. B* 154 (1999) 325.
- [13] T. Wågberg, P. Jacobsson, B. Sundqvist, *Phys. Rev. B* 60 (1999) 4535.
- [14] D. Porezag, M.R. Pederson, Th. Frauenheim, Th. Köhler, *Phys. Rev. B* 52 (1995) 14963.
- [15] R.M. Papaléo, R. Hérino, A. Hallén, P. Demirev, B.U.R. Sundqvist, *Nucl. Instr. and Meth. B* 116 (1996) 274.